

28. F. G. Fuhrman and F. C. Collins, *This Journal*, **124**, 1294 (1977).
29. J. F. Houlihan, R. F. Bonaquist, R. T. Dirstine, and D. P. Madacsi, *Mater. Res. Bull.*, **16**, 659 (1981).
30. J. L. Ord, *This Journal*, **127**, 2682 (1980).
31. N. Sato, *Electrochim. Acta*, **16**, 1683 (1971).
32. See, for example, V. A. Myamlin and Y. V. Pleskov, "Electrochemistry of Semiconductors," Plenum, New York (1967).
33. For a discussion see S. R. Morrison, "Electrochemistry at Semiconductor and Oxidised Metal Electrodes," Plenum, New York (1980).
34. L. M. Peter, *Electrochim. Acta*, **23**, 165 (1978).
35. See, for example, J. A. Harrison and H. R. Thirsk, in "Electroanalytical Chemistry," Vol. 5, A. J. Bard, Editor; Marcel Dekker, New York (1971).
36. F. Möllers, H.-J. Tolle, and R. Memming, *This Journal*, **121**, 1160 (1974).

Electrochemistry and Adsorption of Bis 2,2'-Bipyridinecobalt(I) and Bis 6,6'-Dimethyl-2,2'-Bipyridinecobalt(I) in Acetonitrile

Brian C. Willett* and Fred C. Anson**

Division of Chemistry and Chemical Engineering, Arthur Amos Noyes Laboratories, California Institute of Technology, Pasadena, California 91125

ABSTRACT

Cyclic voltammetry, coulometry, and chronocoulometry were used to examine the reduction of bis-2,2'-bipyridinecobalt(II), $\text{Co}(\text{bipy})_2^{2+}$, and bis-6,6'-dimethyl-2,2'-bipyridinecobalt(II), $\text{Co}(\text{dmbp})_2^{2+}$ in acetonitrile solution. Both of the cobalt(I) reduction products, $\text{Co}(\text{bipy})_2^+$ and $\text{Co}(\text{dmbp})_2^+$, adsorb on mercury but not on graphite or platinum electrodes. $\text{Co}(\text{bipy})_2^+$ decomposes at a modest rate while $\text{Co}(\text{dmbp})_2^+$ is much more stable. Neither reduced complex proved effective as a catalyst for the electroreduction of nitrous oxide or alkyl halides.

In our previous studies of the electrochemical behavior of 2,2'-bipyridine complexes of cobalt(II) and cobalt(I) in acetonitrile solutions the π -coordination of activated olefins by the cobalt(I) complex was investigated (1) and the catalytic reduction of allyl chloride was explored (2). The rate of the catalyzed reduction was greater under conditions where the bis-2,2'-dipyridinecobalt(I) complex, $\text{Co}(\text{bipy})_2^+$, was believed to be the dominant form of the catalyst present. This report concentrates on the preparation and electrochemical behavior of this complex. In contrast with $\text{Co}(\text{bipy})_3^+$, $\text{Co}(\text{bipy})_2^+$ disproportionates fairly rapidly to form unreactive products that limit its utility as an electrocatalyst. However, the analogous Co(I) complex prepared from the more sterically hindered 6,6'-dimethyl-2,2'-bipyridine ligand (dmbp) proved to be much more stable toward disproportionation. The electrochemical behavior of the $\text{Co}(\text{dmbp})_2^{2+}$ complex was therefore also characterized to provide a basis for comparison with that of $\text{Co}(\text{bipy})_2^{2+}$.

Exposure of mercury electrodes to both $\text{Co}(\text{bipy})_2^+$ and $\text{Co}(\text{dmbp})_2^+$ [as well as $\text{Co}(\text{dmbp})_2$] results in very extensive adsorption of the complexes on the electrode surface. Unusual surface coordination and redox chemistries are argued to be responsible for the adsorption.

Experimental

Materials.—"Spectrograde" acetonitrile (Aldrich) was distilled first from CaH_2 and again from BaO just prior to use. (Burdick-Jackson) "U.V. quality" acetonitrile was used as received. "Polarographic grade" tetraethylammonium perchlorate and tetra-*n*-butylammonium perchlorate (Southwestern Analytical Company) were vacuum dried and used as supporting electrolytes without further purification. Tetra-*n*-butylammonium trifluoromethane sulfonate was prepared as described by Brandstrom (3). Sodium perchlorate (G. F. Smith) was recrystallized twice from water and dried at 110°C. Nitrous oxide (Matheson) and *n*-butyl bromide (Matheson, Coleman and Bell) were used as received. $\text{Co}(\text{bipy})_3(\text{ClO}_4)_2$ and $\text{Co}(\text{bipy})_3(\text{ClO}_4)_3 \cdot 3\text{H}_2\text{O}$ were synthesized according to standard pro-

cedures (4). Both salts gave satisfactory elemental analyses as did 6,6'-dimethyl-2,2'-bipyridine, dmbp, synthesized according to a published procedure (5). Elementary analysis of dmbp: C 78.23%; H 6.57%; N 15.21%. Calculated: C 78.45%; H 6.82%; N 15.41%. Solutions of $\text{Co}(\text{bipy})_2^{2+}$ and $\text{Co}(\text{dmbp})_2^{2+}$ were prepared by adding aliquots of a standard solution of $\text{Co}(\text{ClO}_4)_2 \cdot 2\text{H}_2\text{O}$ in acetonitrile to stoichiometric quantities of the ligands in the supporting electrolyte solution just prior to use.

Apparatus.—Cyclic voltammograms were obtained with a Princeton Applied Research (PAR) Model 173 potentiostat driven by a PAR Model 175 universal programmer. Working electrodes were a commercial hanging mercury drop electrode (Metrohm), a static mercury drop electrode (PAR Model 303), a planar platinum button electrode, or a pyrolytic graphite disk electrode mounted in glass with heat-shrinkable tubing.

Chronocoulometry experiments were accomplished by means of a computer-based apparatus similar to that described previously (6). Controlled-potential electrolyses were conducted with the PAR Model 173 potentiostat equipped with a PAR Model 179 digital coulometer. The electrolysis cell employed was modeled after the design described by Moore and Peters (7). Solutions were usually deoxygenated by bubbling with argon that had been passed through hot copper turnings. When more complete exclusion of oxygen was desired, the experiments were connected inside a controlled atmosphere box (Vacuum Atmospheres Company). U.V.-VIS spectra were recorded with a Cary Model 219 Spectrometer or a Hewlett-Packard Model 8450A Spectrometer. Potentials were measured and are reported with respect to an aqueous Ag/AgCl reference electrode, which has a potential ca. 45 mV more negative than a saturated calomel electrode. Experiments were conducted at the laboratory temperature, $22^\circ \pm 3^\circ\text{C}$.

Results and Discussion

$\text{Co}(\text{bipy})_3^{2+}$ and $\text{Co}(\text{bipy})_2^{2+}$.—The cyclic voltammetry of solutions containing cobalt(II) and bipyridine is particularly simple when the molar ratio of metal to ligand is one-to-three. As shown in Fig. 1A, three

* Electrochemical Society Student Member.

** Electrochemical Society Active Member.

Key words: coulometry, chronocoulometry, electroreduction.

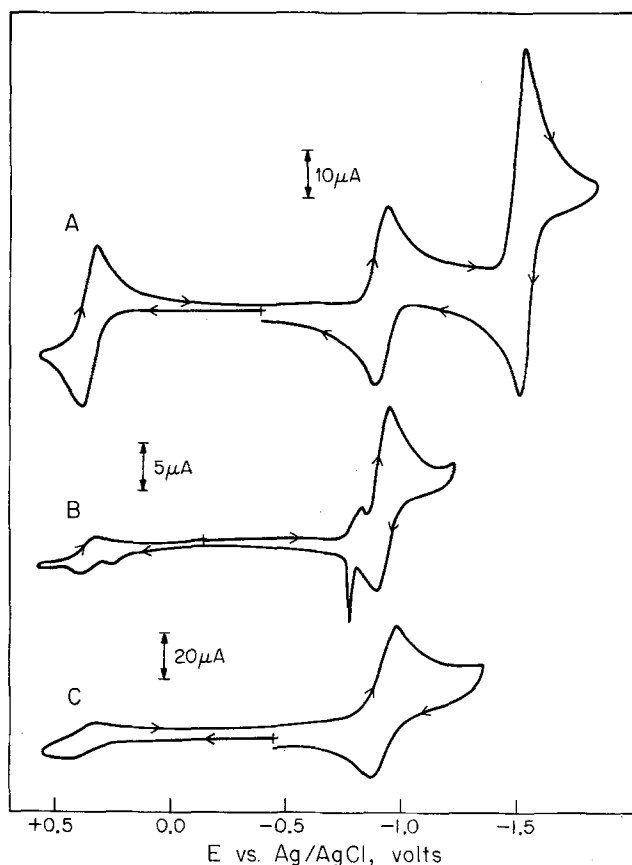


Fig. 1. Cyclic voltammograms of $\text{Co}(\text{bipy})_3^{2+}$ and $\text{Co}(\text{bipy})_2^{2+}$ in acetonitrile. (A) 1.0 mM $\text{Co}(\text{bipy})_3^{2+}$; mercury electrode (0.0255 cm^2); scan rate = 200 mV sec^{-1} . (B) 1.8 mM $\text{Co}(\text{bipy})_2^{2+}$; mercury electrode; scan rate = 100 mV sec^{-1} . (C) 0.5 mM $\text{Co}(\text{bipy})_2^{2+}$; platinum electrode (0.20 cm^2); scan rate = 200 mV sec^{-1} . Supporting electrolyte: A, B— 0.1 M tetraethylammonium perchlorate; C— 0.1 tetrabutylammonium trifluoromethanesulfonate.

waves appear at ca. $+0.4$, -0.9 , and -1.5 V corresponding to the $\text{Co}(\text{III})/\text{Co}(\text{II})$, $\text{Co}(\text{II})/\text{Co}(\text{I})$, and $\text{Co}(\text{I})/(-\text{I})$ couples, respectively (1, 8). The first two couples appear completely reversible at scan rates from 0.02 to 10 Vsec^{-1} while the last couple yields cathodic peak currents that are larger than their anodic counterparts at scan rates below ca. 1 Vsec^{-1} . The responses obtained are essentially identical at both mercury and platinum electrodes. The polarographic half-wave potential for the $\text{Co}(\text{II})/(\text{I})$ couple is unaffected by the addition of as much as 0.1 M excess 2,2'-bipyridine (1) showing that no bipyridine molecules leave the inner coordination sphere of cobalt(II) when it is reduced to cobalt(I).

Double potential step chronocoulometry (9) with solutions of $\text{Co}(\text{bipy})_3^{2+}$ indicate little or no adsorption on mercury or platinum of the tris-bipyridine complexes of cobalt(III), (II), or (I). During controlled-potential reduction of $\text{Co}(\text{bipy})_3^{2+}$, the current decreases exponentially with time and 1.0 faraday per mol of cobalt(II) is consumed. The resulting solutions of $\text{Co}(\text{bipy})_3^+$ are dark blue and appear stable for weeks when stored in an oxygen-free atmosphere.

There are significant changes in this simple pattern when the initial solution contains only 2 mols of 2,2'-bipyridine per mol of cobalt(II). Figures 1B and C show cyclic voltammograms for $\text{Co}(\text{bipy})_2^{2+}$ at mercury and platinum electrodes. At mercury, a small wave appears ahead of the main $\text{Co}(\text{II})$ reduction peak and the corresponding anodic response includes a narrow, sharp wave typical of adsorbed species. In addition, a small irreversible oxidation peak is ob-

served at $+0.14 \text{ V}$ on mercury (its magnitude depends on the scan rate and the concentration of the complex) just prior to the small, reversible response corresponding to the $\text{Co}(\text{II})/(\text{III})$ couple. The magnitude of this $\text{Co}(\text{II})/(\text{III})$ response increases if the ligand-to-cobalt ratio is increased above 2 to 1 and decreases to zero when the ratio is reduced below ca. 1.8 to 1. At any fixed ratio the response gives an indication of the amount of $\text{Co}(\text{bipy})_3^{2+}$ formed by ligand exchange reactions between species with fewer than three coordinated ligands. The irreversible wave at $+0.14 \text{ V}$ arises from the oxidation of cobalt metal as demonstrated by cyclic voltammetry on Hg with solutions of $\text{Co}(\text{ClO}_4)_2 \cdot 2\text{H}_2\text{O}$ in acetonitrile in the absence of bipyridine.

At platinum electrodes, no prewave or anodic spike appear at the potentials where the cobalt(II)/(I) couple is active (Fig. 1C) suggesting that there is much weaker interaction between cobalt(I) and the platinum surface. At both electrodes, the peak current for reduction of $\text{Co}(\text{bipy})_2^{2+}$ exceeds the value for the same concentration of $\text{Co}(\text{bipy})_3^{2+}$ and the ratio of cathodic to anodic peak currents is well above unity. The peak current ratio depends upon the concentration of the complex and the scan rate, approaching unity at sufficiently high scan rates.

The course of controlled-potential reductions of $\text{Co}(\text{bipy})_2^{2+}$ also differs markedly from that of $\text{Co}(\text{bipy})_3^{2+}$; with the latter complex, plots of the logarithm of the current vs. time are linear and 1.0 faraday is consumed per mol of cobalt(II). The former complex yields nonlinear plots and consumes 1.3 - 1.4 faradays per mol. Changes in the color of the electrolysis solution also differ from those observed during the reduction of $\text{Co}(\text{bipy})_3^{2+}$: The initially pale yellow solution develops a violet color during the first few minutes of the electrolysis before it acquires the deep blue color characteristic of $\text{Co}(\text{bipy})_3^+$. No intermediate violet color precedes the appearance of the blue color when $\text{Co}(\text{bipy})_3^{2+}$ is reduced.

Interruption of an electrolysis of $\text{Co}(\text{bipy})_2^{2+}$ at an early stage when the solution is violet results in a fading of the violet color in a matter of minutes and restoration of the initial pale yellow color. [Both $\text{Co}(\text{bipy})_2^{2+}$ and $\text{Co}(\text{bipy})_3^{2+}$ are yellow.] Curve A of Fig. 2 is a spectrum of the violet solution. The spectrum was recorded as rapidly as possible after the electrolysis was interrupted. The spectrum of the stable, blue $\text{Co}(\text{bipy})_3^+$ ion is shown for comparison in curve B. Although the precise composition of the violet solution is uncertain, the spectrum shown is believed to be dominated by $\text{Co}(\text{bipy})_2^+$. [$\text{Co}(\text{bipy})_2^{2+}$

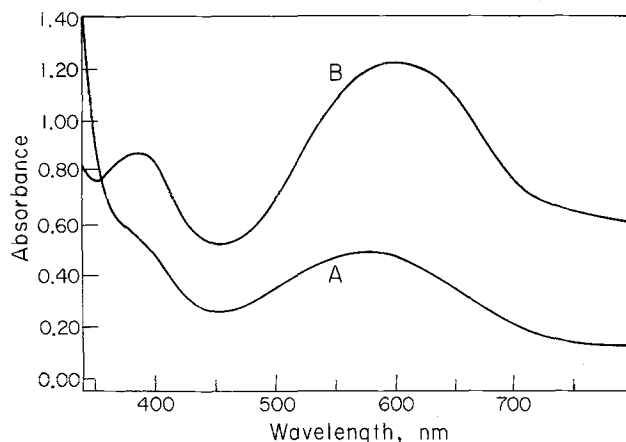
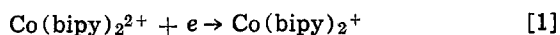
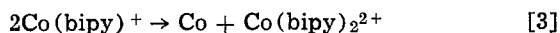
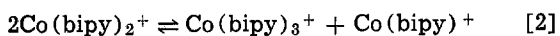
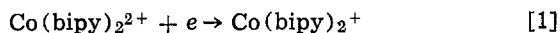


Fig. 2. U.V.-visible spectra of A, $\text{Co}(\text{bipy})_2^+$ and B, $\text{Co}(\text{bipy})_3^+$ in acetonitrile. Spectrum A, obtained from a partially reduced solution of $\text{Co}(\text{bipy})_2^{2+}$, was scaled to correspond to 0.23 mM $\text{Co}(\text{bipy})_2^+$. Spectrum B is for a 0.23 mM solution of $\text{Co}(\text{bipy})_3^{2+}$ that was fully reduced to $\text{Co}(\text{bipy})_3^+$.

and $\text{Co}(\text{bipy})_3^{2+}$ absorb negligibly at wavelengths greater than 450 nm; the only likely interfering contaminant is $\text{Co}(\text{bipy})_3^+$ and none was detected in the spectrum obtained after the violet color had disappeared.]

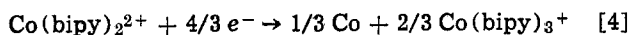
Solutions of $\text{Co}(\text{bipy})_2^{2+}$ that have been exhaustively electrolyzed at -1.2V have spectra that are identical to that of $\text{Co}(\text{bipy})_3^+$, but only two-thirds of the initial cobalt is accounted for by the intensity of the absorption. Cyclic voltammograms show a reversible response at the potential corresponding to the $\text{Co}(\text{bipy})_3^{2+}/\text{Co}(\text{bipy})_3^+$ couple with peak currents corresponding to two-thirds of the cobalt initially present. The missing cobalt cannot be recovered by the addition of more bipyridine. It is believed to be in the form of cobalt metal that results from the decomposition of cobalt(I) complexes containing fewer than two bipyridine ligands, as outlined in Scheme I

SCHEME I



etc.

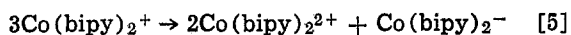
According to this scheme the net result of the electrolysis of a solution of $\text{Co}(\text{bipy})_2^{2+}$ will be given by reaction [4]



This accounts for both the observed disappearance of one-third of the cobalt and the consumption of 1.3-1.4 faradays per mol of cobalt during the electrolysis.

Scheme I also accounts for the observation that the cathodic peak currents in cyclic voltammograms of 1 mM solutions of $\text{Co}(\text{bipy})_2^{2+}$ exceed the anodic peak currents except at scan rates above *ca.* 2Vsec^{-1} . Additional support for Scheme I comes from the observation that voltammograms obtained in solutions prepared by adding equimolar quantities of Co^{2+} and bipyridine to acetonitrile show new peaks that correspond to the deposition of cobalt metal as well as smaller peaks for the generation of $\text{Co}(\text{bipy})_2^+$.

An alternative scheme can be written for the loss of $\text{Co}(\text{bipy})_2^+$ involving its disproportionation to $\text{Co}(\text{bipy})_2^0$ and $\text{Co}(\text{bipy})_2^{2+}$. However, Groshens *et al.* (10) have examined the electrochemistry of chemically synthesized $\text{Co}(\text{bipy})_2^0$ and shown that it is thermodynamically unstable with respect to disproportionation to $\text{Co}(\text{bipy})_2^+$ and $\text{Co}(\text{bipy})_2^-$ [as is consistent with the absence of a wave for the reduction of $\text{Co}(\text{bipy})_2^+$ to $\text{Co}(\text{bipy})_2^0$ in the cyclic voltammetry of $\text{Co}(\text{bipy})_2^{2+}$]. Thus, the disproportionation of $\text{Co}(\text{bipy})_2^+$ would have to proceed according to reaction [5]



and the equilibrium constant for this reaction can be calculated from the relevant voltammetric peak potentials (10) to be *ca.* 10^{-40} . This is one reason that the observed decomposition of $\text{Co}(\text{bipy})_2^+$ was ascribed to reactions such as those given in Scheme I instead of to direct disproportionation as depicted in reaction [5].

$\text{Co}(\text{bipy})_2^+$ generated by the disproportionation of $\text{Co}(\text{bipy})_2^0$ should also decompose via reactions [2] and [3] of Scheme I. Groshens *et al.* (10) did not consider this possibility but the cyclic voltammograms they report for solutions prepared from $\text{Co}(\text{bipy})_2^0$ contain prominent peaks at the potential of the $\text{Co}(\text{III})/\text{Co}(\text{II})$ couple and we have found that these

peaks only appear when tris bipyridine complexes are present (Fig. 1). In addition, the peak current densities of the voltammograms shown in Ref. (10) are about half as great as those that we and Groshens *et al.* [cf. Fig. 2A of Ref. (10)] observe under the same conditions when the solution is prepared from $\text{Co}(\text{bipy})_2^{2+}$. The conductance of solutions prepared from $\text{Co}(\text{bipy})_2^0$ (10) is also much smaller than would be expected if all of the cobalt added were present as $\text{Co}(\text{bipy})_2^+$ and $\text{Co}(\text{bipy})_2^-$. Thus, we conclude that the disproportionation of $\text{Co}(\text{bipy})_2^0$ in acetonitrile to yield $\text{Co}(\text{bipy})_2^+$ and $\text{Co}(\text{bipy})_2^-$ as described in Ref. (10) was accompanied by significant decomposition of the $\text{Co}(\text{bipy})_2^+$ so that Co and $\text{Co}(\text{bipy})_3^+$ were also produced by reactions [2] and [3] of Scheme I.

Reactions of $\text{Co}(\text{bipy})_2^+$ with reducible substrates.—One objective in studying the electrochemical reduction of $\text{Co}(\text{bipy})_2^{2+}$ was the possibility that $\text{Co}(\text{bipy})_2^+$, with an open coordination site, would prove to be a better catalyst than $\text{Co}(\text{bipy})_3^+$ for reductions of substrates that are difficult to reduce directly but might be activated by coordination to the $\text{Co}(\text{I})$ centers. Nitrous oxide was examined as a possible substrate because its reduction by borohydride in homogeneous solution is known to be catalyzed by cobalt-bipyridine complexes (11) and the direct electrochemical reduction of N_2O at mercury occurs at potentials much more negative than those where $\text{Co}(\text{bipy})_2^{2+}$ is reduced (12).

Cyclic voltammograms for the $\text{Co}(\text{bipy})_3^{2+}$ and $\text{Co}(\text{bipy})_2^{2+}$ in the absence and presence of N_2O are compared in Fig. 3. The addition of N_2O produces very little change in the peak currents for the reduction of either complex. However, the anodic peak currents are decreased significantly and the bigger effect is shown by $\text{Co}(\text{bipy})_2^{2+}$. The addition of N_2O also eliminates the adsorption pre- and post-waves ex-

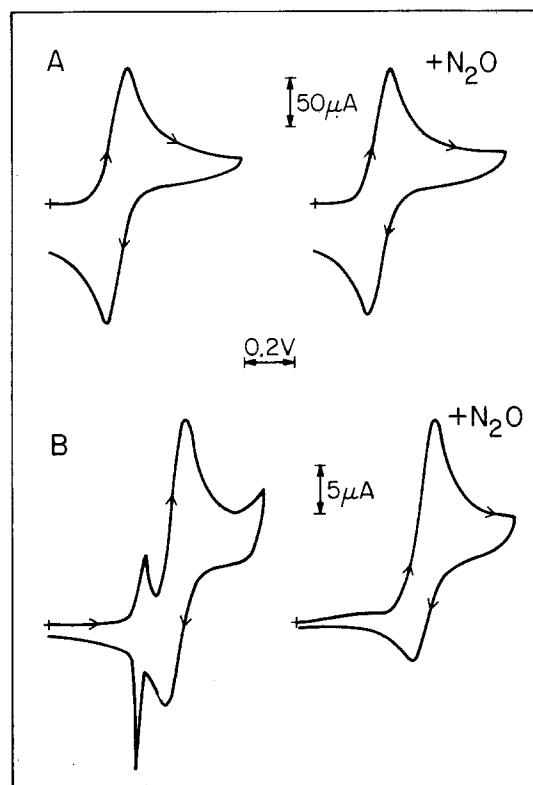


Fig. 3. Effect of N_2O on cyclic voltammograms of $\text{Co}(\text{bipy})_2^{2+}$ and $\text{Co}(\text{bipy})_3^{2+}$. (A) 1.9 mM $\text{Co}(\text{bipy})_3^{2+}$; platinum electrode; initial potential -0.6V . (B) 2.0 mM $\text{Co}(\text{bipy})_2^{2+}$; mercury electrode; initial potential -0.4V . Supporting electrolyte: 0.1M tetraethylammonium perchlorate. Scan rate = 200mV sec^{-1} .

hibited by $\text{Co}(\text{bipy})_2^{2+}$ at mercury electrodes. Chronocoulometric tests showed that the adsorption of the reduced complex is essentially eliminated by the addition of N_2O .

The lack of significant increases in the cathodic peak currents in Fig. 3 in the presence of N_2O shows that the rate of reaction between $\text{Co}(\text{bipy})_3^+$ or $\text{Co}(\text{bipy})_2^+$ and N_2O is not large under these conditions. However, the decrease in anodic current suggests that N_2O does react with $\text{Co}(\text{bipy})_2^+$ [but not $\text{Co}(\text{bipy})_3^+$] either to form a moderately stable adduct that is not oxidizable at potentials where $\text{Co}(\text{bipy})_2^+$ is oxidized or to produce oxide (or hydroxide) ion that attacks the $\text{Co}(\text{bipy})_2^+$ complex¹ thus decreasing the anodic peak current. The reaction also reduces the adsorption of $\text{Co}(\text{bipy})_2^+$ suggesting that, if an adduct is formed, the coordination site at $\text{Co}(\text{I})$ that is occupied by the N_2O is essential for the formation of the adsorption bond to the mercury surface.

Repeated cycling of the mercury electrode in solutions of $\text{Co}(\text{bipy})_2^{2+}$ and N_2O causes the voltammogram to collapse until almost no current flows. The response returns immediately at a fresh electrode. At a platinum electrode the voltammogram collapses almost immediately, indicating a strong passivation of the electrode surface. Similar behavior results during controlled potential reductions of $\text{Co}(\text{bipy})_2^{2+}$ at -1.2V in the presence of excess N_2O . The electrolysis current does not attain a steady level as would be expected if a catalytic reduction of the N_2O were proceeding. Instead the current decays [plots of $\log(\text{current})$ vs. time are nonlinear] reaching zero after ca. 1.7 faradays per mol of cobalt are passed through the solution. The resulting brownish-yellow solution contains a small quantity of a dark precipitate and exhibits no electrochemical responses at a fresh mercury drop electrode except for an anodic wave attributable to the presence of free bipyridine. It seems likely that the oxide ion (or hydroxide ion) generated by the slow reduction of N_2O to N_2 attacks the cobalt-bipyridine complexes present, removing the cobalt from solution and thereby halting the electrolysis. The substance produced by the reaction with the strong base is believed to form stable, passivating coatings on the surfaces of mercury and platinum electrodes that are responsible for the rapid decay in the current. The electrolysis could be prolonged a little by addition of proton donors but we were unable to find conditions where the $\text{Co}(\text{bipy})_2^+$ -facilitated reduction of N_2O could be sustained.

With substrates whose reduction does not liberate a strong base, e.g., alkyl halides, $\text{Co}(\text{bipy})_2^+$ could conceivably serve as an effective reduction catalyst. However, the catalytic reaction would have to proceed relatively rapidly in order to avoid the loss of catalyst according to Scheme I with precipitation of cobalt metal. This was the case with allyl chloride (2) but with nonactivated halides, e.g., n-butylbromide, the reaction with $\text{Co}(\text{bipy})_2^+$ was too slow to be practical for electrosynthetic exploitation.

Bis 6,6'-dimethyl-2,2'-bipyridine cobalt(II).—A cyclic voltammogram for $\text{Co}(\text{dmbp})_2^{2+}$ recorded at a pyrolytic graphite electrode is shown in Fig. 4A while 4B shows the response obtained at a mercury electrode. The reversible couples at -0.63 and -1.20V both correspond to one-electron processes, i.e., $\text{Co}(\text{II}) \rightleftharpoons \text{Co}(\text{I})$ and $\text{Co}(\text{I}) \rightleftharpoons \text{Co}(\text{0})$. The anodic wave at $+0.32\text{V}$ is observed only at mercury and is therefore not attributable to the oxidation of $\text{Co}(\text{II})$ to $\text{Co}(\text{III})$. Instead, the wave is believed to arise from the oxida-

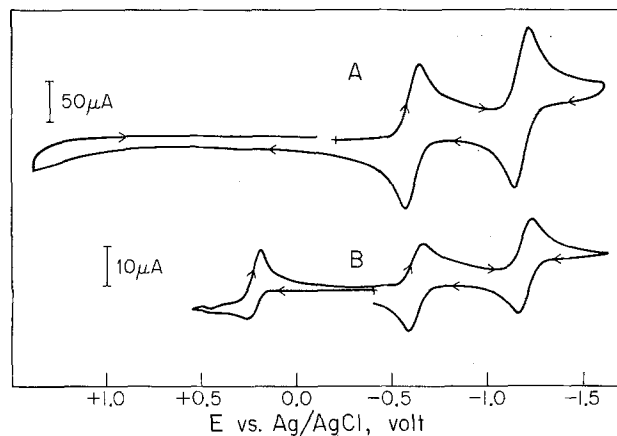


Fig. 4. Cyclic voltammogram of 1.8 mM $\text{Co}(\text{dmbp})_2^{2+}$ in acetonitrile. (A) Pyrolytic graphite electrode. (B) Mercury electrode. Scan rate: 100 mV sec^{-1} . Supporting electrolyte: 0.1M tetraethylammonium perchlorate.

tion of mercury to form $\text{Hg}(\text{dmbp})_2^{2+}$ and Co^{2+} . The same wave appears in solutions containing only the uncoordinated ligand but its peak potential appears at a less positive value ($+0.26\text{V}$), as expected. No corresponding anodic wave is present in solutions of $\text{Co}(\text{bipy})_2^{2+}$ [or $\text{Co}(\text{bipy})_3^{2+}$] probably because of the much greater stability (and/or smaller lability) of this complex.

No wave for the oxidation of $\text{Co}(\text{II})$ to $\text{Co}(\text{III})$ was found under any conditions at graphite or platinum electrodes, even in the presence of 10 mM uncoordinated ligand at potentials as positive as $+1.5\text{V}$. The two methyl substituents apparently produce sufficient steric crowding to prevent the formation of the tris complex that would be required for the oxidation of $\text{Co}(\text{II})$ to $\text{Co}(\text{III})$ to proceed at accessible potentials.

The ratio of anodic to cathodic peak currents for the $\text{Co}(\text{II})/(\text{I})$ and $\text{Co}(\text{I})/(\text{0})$ waves in Fig. 4A are close to 1.0 at all scan rates, indicating that both of the reduced forms of the complex are much more stable than is $\text{Co}(\text{bipy})_2^+$. This was confirmed by controlled-potential reduction of a solution of $\text{Co}(\text{dmbp})_2^{2+}$ at -0.9V . Linear $\log(\text{current})$ vs. time curves resulted and 1.05 faradays were consumed per mol of complex. The resulting purple solution showed no evidence of decomposition by pathways similar to those in Scheme I. It was stable for days in the absence of oxygen. A spectrum of a solution of $\text{Co}(\text{dmbp})_2^+$ is given in Fig. 5, curve A.

Further reduction of $\text{Co}(\text{dmbp})_2^+$ at -1.5V consumed an additional 1.07 faradays per mol of complex

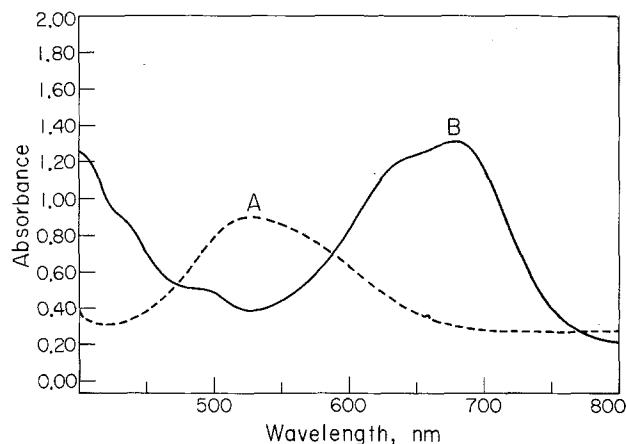


Fig. 5. U.V.-visible spectra of 0.23 mM solutions of (A) $\text{Co}(\text{dmbp})_2^+$ and (B) $\text{Co}(\text{dmbp})_2$ in acetonitrile.

¹ Addition of tetramethylammonium hydroxide to acetonitrile solutions of $\text{Co}(\text{bipy})_3^{2+}$ or $\text{Co}(\text{bipy})_2^{2+}$ causes the yellow color to fade. The only cyclic voltammetric response in the resulting solutions appears at potentials where mercury is oxidized in the presence of free bipyridine.

and produced a dark blue-black solution whose spectrum is shown in Fig. 5, curve B. This reduced solution appeared stable for several hours in the absence of oxygen but cobalt metal precipitated from the solution if it was allowed to stand overnight.

Exposure of $\text{Co}(\text{dmbp})_2^{2+}$ to reducible substrates.—The formal potential of the $\text{Co}(\text{dmbp})_2^{2+}/+$ couple is about 400 mV more positive than that of the $\text{Co}(\text{bipy})_2^{2+}/+$ couple. $\text{Co}(\text{dmbp})_2^{2+}$ is thus a much weaker reductant than $\text{Co}(\text{bipy})_2^{2+}$ and this is reflected in its inertness toward potentially reducible substrates. Addition of nitrous oxide to solutions of $\text{Co}(\text{dmbp})_2^{2+}$ produced no detectable changes in the cyclic voltammogram for the $\text{Co}(\text{dmbp})_2^{2+}/+$ couple. In particular, and in contrast with the $\text{Co}(\text{bipy})_2^{2+}/+$ couple, the anodic peak current was undiminished and the anodic peak potential did not shift in the presence of N_2O . This indicates that N_2O does not coordinate with $\text{Co}(\text{dmbp})_2^{2+}$ (and it is certainly not reduced at an appreciable rate). Supporting this interpretation was the failure of N_2O to affect the adsorption of $\text{Co}(\text{dmbp})_2^{2+}$ (*vide infra*) in the way that it did for $\text{Co}(\text{bipy})_2^{2+}$.

Even the cyclic voltammogram corresponding to the reduction of $\text{Co}(\text{dmbp})_2^{2+}$ to $\text{Co}(\text{dmbp})_2^0$ was largely unaffected by the addition of N_2O . The only change was a small ($\sim 10\%$) decrease in the anodic peak current suggesting weak coordination of N_2O to the cobalt(0) complex but no further reaction on the time scale of the cyclic voltammetric experiment (~ 30 sec).

Adsorption of $\text{Co}(\text{bipy})_2^{2+}$ on mercury.—Chronocoulometry (9) showed no detectable adsorption ($< 10^{-11}$ mols cm^{-2}) of $\text{Co}(\text{bipy})_2^{2+}$ on mercury or platinum electrodes. However, there was clear evidence for strong adsorption when mercury (but not platinum) electrodes were exposed to $\text{Co}(\text{bipy})_2^{2+}$. Because of the relatively rapid decomposition of $\text{Co}(\text{bipy})_2^{2+}$ (Scheme I), it was not possible to prepare stable solutions in which the adsorption could be measured. Instead, solutions of $\text{Co}(\text{bipy})_2^{2+}$ were employed and $\text{Co}(\text{bipy})_2^{2+}$ was generated at the electrode surface by adjusting its potential to -1.2V where the diffusion-limited reduction of $\text{Co}(\text{bipy})_2^{2+}$ proceeded. At the end of the generation period (45 sec was typical), the electrode potential was stepped to -0.4V where the diffusion-limited oxidation of $\text{Co}(\text{bipy})_2^{2+}$ proceeded. The resulting charge-time data were linearized by plotting charge vs. $(\text{time})^{1/2}$ (9) and the quantity of $\text{Co}(\text{bipy})_2^{2+}$ adsorbed was estimated from the difference between the charge axis intercept and the corresponding value measured in a blank run in the pure supporting electrolyte. The slopes of the chronocoulometric plots of charge vs. $(\text{time})^{1/2}$ were typically about half as large as those obtained in corresponding experiments in which the stable $\text{Co}(\text{bipy})_3^{2+}$ complex was generated at the electrode and then reoxidized to $\text{Co}(\text{bipy})_3^{2+}$. The smaller slopes almost certainly result from the partial decomposition of $\text{Co}(\text{bipy})_2^{2+}$ during the period that it is generated. This means that the actual interfacial concentrations of $\text{Co}(\text{bipy})_2^{2+}$ that give rise to the adsorption cannot be measured precisely. In presenting the adsorption data we have therefore elected to specify the concentrations of the $\text{Co}(\text{bipy})_2^{2+}$ solutions in which the $\text{Co}(\text{bipy})_2^{2+}$ was generated with the understanding that this provides only a qualitative measure of the effect of concentration changes on the adsorption.

Table I summarizes the adsorption data at several concentrations of $\text{Co}(\text{bipy})_2^{2+}$. The adsorption is clearly quite extensive, even from 0.1 mM solutions. The apparent maximum in the adsorption at a concentration of 0.45 mM may be the result of competition between the adsorbate and the increasing quantities of cobalt metal that are deposited on the mercury

Table I. Adsorption on mercury of the product of the reduction of $\text{Co}(\text{bipy})_2^{2+}$ in acetonitrile^{a,b}

Concentration of $\text{Co}(\text{bipy})_2^{2+}$, mM	$n\Gamma$, μC^c
0.11	12
0.14	16
0.23	42
0.45	100
0.9	78
1.8	78
3.6	88

^a Supporting electrolyte: 0.1M tetrabutylammonium trifluoromethanesulfonate.

^b The electrode potential was held for 45 sec at -1.2V and then stepped to -0.4V for 100 msec.

^c To convert these values into mol cm^{-2} , $n = 2$ should be used (see text).

surface via reactions [2] and [3] as the concentration of $\text{Co}(\text{bipy})_2^{2+}$ increases.

Chronocoulometric charge-time transients for the reduction of $\text{Co}(\text{bipy})_2^{2+}$ are strongly influenced by the fact that the $\text{Co}(\text{bipy})_2^{2+}$ formed at the electrode is adsorbed. Figure 6 shows that the slope of the charge- $(\text{time})^{1/2}$ plot at times before the adsorption has attained its final value is larger for the reduction of $\text{Co}(\text{bipy})_2^{2+}$ than of $\text{Co}(\text{bipy})_3^{2+}$ where there is little or no adsorption of the reaction product. Chronocoulometric charge- $(\text{time})^{1/2}$ transients for electrode processes in which an unadsorbed reactant is converted to an adsorbed product are usually no different from those obtained without product adsorption unless the adsorption results in large changes in the electric charge density on the electrode surface. The differential capacitance of the mercury electrodes at -1.2V showed no major increase in the presence of $\text{Co}(\text{bipy})_2^{2+}$ so that the higher slope of curve B in Fig. 6 cannot be attributed to changes in the surface charge density of the electrode. Instead, we believe the higher initial slope results from the further reduction of $\text{Co}(\text{bipy})_2^{2+}$ by one electron as it is adsorbed. Thus the $\text{Co}(\text{bipy})_2^{2+}$ that is reduced to adsorbed product consumes two electrons while only one electron is consumed in reducing unadsorbed $\text{Co}(\text{bipy})_2^{2+}$ to unadsorbed $\text{Co}(\text{bipy})_2^{2+}$. The higher slope decreases toward the value expected for a one-electron reduction once the electrode surface is fully covered with the adsorbed product because continued reduction of $\text{Co}(\text{bipy})_2^{2+}$ requires only one electron. Supporting this interpretation are the data in Table II, which show that the ratio

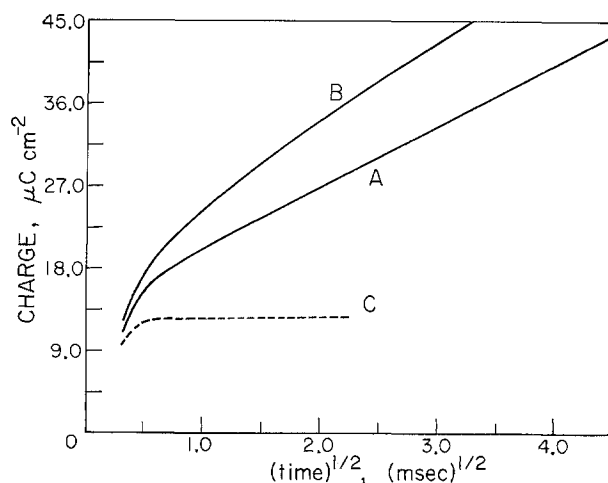


Fig. 6. Chronocoulometric charge- $(\text{time})^{1/2}$ transients for the reduction of (A) $\text{Co}(\text{bipy})_3^{2+}$ and (B) $\text{Co}(\text{bipy})_2^{2+}$ at mercury electrodes. The potential was stepped from -0.4 to -1.2V . (C) Response obtained in the pure supporting electrolyte. Supporting electrolyte as in Fig. 1B.

Table II. Ratio of slopes of charge-(time)^{1/2} plots for the reductions of Co(bipy)₃²⁺ and Co(bipy)₂²⁺ at mercury electrodes in acetonitrile^a

Concentration of complex, mM	Slope ratio ^b	nFΓ/Q _{tot} ^c
0.11	1.32	0.30
0.14	1.28	0.26
0.23	1.28	0.27
0.45	1.20	0.28
0.90	1.21	0.26
1.8	1.12	0.17
3.6	1.07	0.12

^a The potential was stepped from -0.4 to -1.2V for 100 msec. The slopes were obtained from a least-squares fit of the charge-time data. Supporting electrolyte as in Table I.

^b Slope for Co(bipy)₃²⁺

^c Slope for Co(bipy)₂²⁺

^c nFΓ is the quantity of cobalt complex adsorbed at the end of 100 msec. It was estimated from the faradaic charge consumed in the first 0.2 msec after the potential was stepped from -1.2V back to -0.4V; Q_{tot} is the total faradaic charge passed during the recording of the charge-time transient.

of the initial slopes of chronocoulometric plots for the reduction of Co(bipy)₂²⁺ and Co(bipy)₃²⁺ depends on the reactant concentration. The ratio approaches unity as the concentration increases because a smaller and smaller fraction of Co(bipy)₂²⁺ generated at the electrode surface is adsorbed.

According to this interpretation, the species adsorbed is a complex of Co(0). The fact that the adsorption occurs on mercury but not on platinum or graphite electrodes indicates that the adsorption requires strong interaction with the mercury atoms on the electrode surface. A stabilizing interaction with the surface would also be required to overcome the intrinsic instability of Co(bipy)₂⁰ demonstrated by Groshens *et al.* (10). Increasing the d electron density on the cobalt by reduction to cobalt(0) would be expected to favor the formation of a metal-metal bond with mercury. Similar surface coordination chemistry leading to adsorption on mercury was encountered in previous studies with low-valent complexes of cobalt (13) and rhodium (14).

If two electrons are involved in the oxidation of the adsorbed cobalt complex, the molar quantities adsorbed are only half as great as might have been anticipated from the data of Table I. Nevertheless, the maximum quantities adsorbed represent more of the complex than could be accommodated in a close-packed monolayer with the bipyridine rings positioned parallel to the surface [ca. 1.5 × 10⁻¹⁰ mols cm⁻² for a molecular diameter of 14Å (15)]. Adsorption with the bipyridine rings perpendicular to the electrode surface is conceivable, especially if the resulting "stack" of bipyridine ligands could interact cooperatively with one another because the very strong dependence of the adsorption on concentration (Table I) points to attractive rather than repulsive interactions between the adsorbing molecules.

The potential dependence of the adsorption was not clearly established because measurements were restricted to a narrow range of potentials by the proximity of the wave corresponding to the further reduction of Co(bipy)₂²⁺. A weak trend toward increased adsorption at more negative potentials appeared to be present. This might reflect the fact that the adsorption of Co(bipy)₂²⁺ is accompanied by its reduction; a step that proceeds only at more negative potentials in the absence of adsorption.

Addition of nitrous oxide or acrylonitrile to solutions of Co(bipy)₂²⁺ greatly diminished the adsorption of subsequently generated Co(bipy)₂²⁺. Both of these molecules are likely to coordinate to the Co(bipy)₂²⁺ complex (2), where they may block the position needed for the formation of the mercury-cobalt bond believed to be responsible for the adsorption.

The interpretation offered here for the pattern of adsorption exhibited by Co(bipy)₂²⁺ is supported by the adsorption behavior of the analogous cobalt complex of 6,6'-dimethyl-2,2'-bipyridine as discussed in the following section.

Adsorption of Co(dmbp)₂²⁺ on mercury.—Although the cyclic voltammograms for Co(dmbp)₂²⁺ (Fig. 4B) contain none of the hallmarks of adsorption evident in the voltammograms of Co(bipy)₂²⁺ (Fig. 1B), chronocoulometric measurements revealed extensive adsorption of Co(dmbp)₂²⁺. The greater stability of Co(dmbp)₂²⁺ [compared with Co(bipy)₂²⁺] simplified the measurement of its adsorption on mercury. The complex was generated at the electrode surface in solutions of Co(dmbp)₂²⁺ by adjusting the electrode potential to values between the Co(dmbp)₂^{2+/+} and Co(dmbp)₂^{2+/0} waves for 45 sec before stepping to -0.1V where the complex was reoxidized to Co(dmbp)₂²⁺ at a diffusion-controlled rate. The plots of anodic charge vs. (time)^{1/2} had slopes that matched those for the corresponding steps for the reduction of Co(dmbp)₂²⁺ showing that Co(dmbp)₂²⁺ was not disproportionating. In addition, the plots for the reduction of Co(dmbp)₂²⁺ did not show the higher slopes exhibited in the analogous experiments with Co(bipy)₂²⁺. This indicates that the reduction of Co(dmbp)₂²⁺ to both adsorbed and unadsorbed Co(dmbp)₂²⁺ consumes only one electron and serves to support the previous interpretation of the higher slopes of the charge-(time)^{1/2} plots for Co(bipy)₂²⁺. The extent of adsorption of Co(dmbp)₂²⁺, determined from the intercepts of charge-(time)^{1/2} plots for the step to -0.1V, is shown in Fig. 7A as a function of the

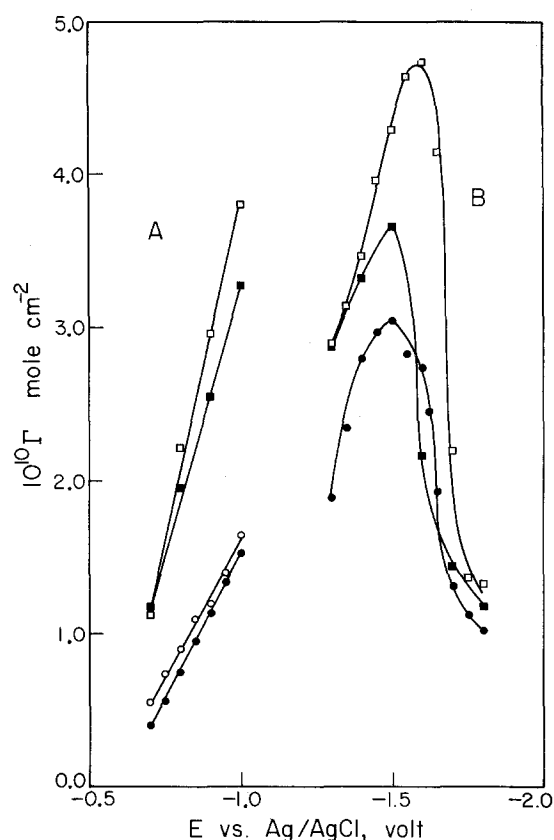


Fig. 7. Potential dependence of the adsorption of (A) Co(dmbp)₂²⁺ and (B) Co(bipy)₂²⁺ at mercury electrodes. The electrode was held for 45 sec at the indicated potential in a solution of Co(dmbp)₂²⁺ and then stepped to -0.1V for 100 msec. Concentration of Co(dmbp)₂²⁺, mM: ●, 0.11; ○, 0.23; ■, 0.45; □, 0.90. Supporting electrolyte: 0.1M tetrabutylammonium trifluoromethanesulfonate.

potential where the $\text{Co}(\text{dmbp})_2^+$ was generated. The adsorption was measured over a sufficiently wide range of potentials to establish clearly that the adsorption increases at more negative potentials. Since no further reduction accompanies the adsorption of $\text{Co}(\text{dmbp})_2^+$, the potential dependence must have a different origin than that suggested earlier for the case of $\text{Co}(\text{bipy})_2^+$. The adsorbing species is cationic but the dependence seems too strong to be attributed to simple electrostatic factors. Studies of metal-metal bonding in the adsorption of low valent transition metal complexes are still too sparse to provide a basis for understanding the effect of electrode potential on the extent of adsorption. At the highest concentrations and most negative potentials, the adsorption reaches values almost as large as those obtained with $\text{Co}(\text{bipy})_2^+$ and it clearly exceeds the value corresponding to a monolayer of complexes lying flat on the electrode.

The adsorption of $\text{Co}(\text{dmbp})_2$ was also measured chronocoulometrically by generating this complex at the electrode surface in solutions of $\text{Co}(\text{dmbp})_2^{2+}$. The results, displayed in Fig. 7B, show an even stronger potential dependence of the adsorption that passes through a rather sharp maximum. The decrease in adsorption at the most negative potentials could arise from preferential adsorption of the supporting electrolyte cations but the factors underlying the large increase in adsorption at potentials positive of the maximum are not evident.

Conclusions

This study has pointed to the intrinsic reactivity of $\text{Co}(\text{bipy})_2^+$ that originates in its coordinative unsaturation and is expressed by its search for an additional ligand (Scheme I) and by its strong interactions with the surface of mercury electrodes. Our original hopes that the reactivity of the ion might also allow it to be exploited as an active catalyst were not fulfilled. The complex is not effective as a catalyst for the reduction of N_2O or alkyl halides. The related complex, $\text{Co}(\text{dmbp})_2^+$, is much more stable than $\text{Co}(\text{bipy})_2^+$ and strongly adsorbed on mercury, but even less reactive toward alkyl halides and N_2O . The adsorption of both complexes is proposed to depend upon the formation of cobalt-mercury bonds and in the case of $\text{Co}(\text{bipy})_2^+$, further reduction accom-

panies adsorption so that the species adsorbed is a complex of $\text{Co}(0)$.

Acknowledgments

This work was supported by the National Science Foundation. Helpful discussions with Professor Duane Bartak are a pleasure to acknowledge. Initial exploratory experiments by Dr. Roger Sperline aided and guided us in portions of the work described here.

Manuscript submitted Oct. 5, 1981; revised manuscript received Dec. 14, 1981.

Any discussion of this paper will appear in a Discussion Section to be published in the December 1982 JOURNAL. All discussions for the December 1982 Discussion Section should be submitted by Aug. 1, 1982.

Publication costs of this article were assisted by the California Institute of Technology.

REFERENCES

1. S. Margel, W. Smith, and F. C. Anson, *This Journal*, **125**, 241 (1978).
2. S. Margel and F. C. Anson, *ibid.*, **125**, 1232 (1978).
3. A. Brandstrom, *Acta Chem. Scand.*, 3585 (1969).
4. F. H. Burstall and N. S. Nyholm, *J. Chem. Soc.*, 3570 (1952).
5. T. Kauffman, J. Konig, and A. Woltermann, *Chem. Ber.*, **109**, 3864 (1976).
6. G. Lauer, R. Abel, and F. C. Anson, *Anal. Chem.*, **39**, 765 (1967).
7. H. M. Moore and D. G. Peters, *J. Am. Chem. Soc.*, **97**, 139 (1975).
8. N. Tanaka and Y. Sato, *Bull. Chem. Soc. Jpn.*, **41**, 2059 (1968).
9. J. H. Christie, R. A. Osteryoung, and F. C. Anson, *J. Electroanal. Chem. Interfacial Electrochem.*, **13**, 236 (1967).
10. T. G. Groshens, B. Henne, D. Bartak, and K. J. Klabunde, *Inorg. Chem.*, **20**, 3629 (1981).
11. R. Banks, R. Henderson, and J. Pratt, *Chem. Commun.*, 387 (1967).
12. Z. Zagorski and J. Suwalski, *J. Electroanal. Chem. Interfacial Electrochem.*, **46**, 353 (1973).
13. H. S. Lim and F. C. Anson, *ibid.*, **31**, 297 (1971).
14. J. Gulens, D. Konrad, and F. C. Anson, *This Journal*, **121**, 1421 (1974).
15. (a) T. Saji and S. Aoyagui, *Bull. Chem. Soc. Jpn.*, **46**, 2101 (1973); (b) R. C. Young, F. R. Keene, and T. J. Meyer, *J. Am. Chem. Soc.*, **99**, 2468 (1977).

Technical Note



Magnetic Field Effects on the Growth of the Diffusion Layer at Vertical Electrodes during Electrodeposition

R. N. O'Brien

Department of Chemistry, University of Victoria, Victoria, BC, Canada

and K. S. V. Santhanam

Chemical Physics Group, Tata Institute of Fundamental Research, Bombay, India

Free or natural convection has been long studied and descriptive equations have been evolved (1-4). The earliest reported interferometric observation of natural

Key words: interferometry, convection, magnetic field, concentration gradients.

convection was by O'Brien, Yakymshyn, and Leja (5) in microcells where the usual electrode area to electrolyte volume ratio of about 1/500 was raised to about 10/1. Electrodes were studied in several orientations. Horizontal electrodes with the cathode over the anode